CD47 antibody protects mice from doxorubicin-induced myocardial damage by suppressing cardiomyocyte apoptosis

YAN HAO[1], LIANGHUA CHEN[1] and ZHILONG JIANG[2]

[1]Department of Cardiology, Shandong Provincial Hospital Affiliated to Shandong First Medical University, Jinan, Shandong 250021; [2]Department of Pulmonary Medicine, Zhongshan Hospital Affiliated to Fudan University, Shanghai 200032, P.R. China

Received September 8, 2021; Accepted March 4, 2022

DOI: 10.3892/etm.2022.11277

Abstract. Cluster of differentiation 47 (CD47) is upregulated in mouse models of doxorubicin (Dox)-induced dilated cardiomyopathy (DCM). To explore the role of CD47 in the development of DCM, in the present study, CD47 signaling was blocked by an anti-CD47 neutralizing antibody (aCD47) in mice with Dox-induced DCM. Intraperitoneal (i.p.) administration of 10 mg/kg Dox once a week significantly induced the development of DCM after 4 weeks, which was accompanied by the upregulation of CD47 expression in heart tissues. However, co-administration of Dox with 7 mg/kg aCD47 once a week significantly reduced the severity of DCM, with lower numbers of disordered and broken myofibers, reduced cardiomyocytes and infiltration of macrophages in the heart tissues of treated mice. The beneficial effects were associated with the reduced population of Annexin $V^+7\text{-}AAD^-$ apoptotic cells, and the attenuated formation of interstitial fibrosis and release of lactate dehydrogenase (LDH) in the aCD47-treated mice. In addition, co-administration with aCD47 effectively reduced the expression of Bax, collagen I, interleukin (IL)-6 and tumor necrosis factor (TNF)-α in murine DCM. These results were further supported by an *in vitro* study, in which aCD47 pre-treatment significantly reduced the Dox-induced early apoptosis of cardiomyocytes and suppressed the expression of Bax, cleaved caspase-1/3 and phosphorylation of p38 MAPK. Therefore, aCD47 attenuated DCM in mice, possibly by suppressing cardiomyocyte early apoptosis and p38 MAPK signaling. CD47 may be a useful therapeutic target in the treatment of DCM.

Correspondence to: Dr Zhilong Jiang, Department of Pulmonary Medicine, Zhongshan Hospital Affiliated to Fudan University, 180 Feng Lin Road, Shanghai 200032, P.R. China
E-mail: jiang.zhilong@zs-hospital.sh.cn

Dr Lianghua Chen, Department of Cardiology, Shandong Provincial Hospital Affiliated to Shandong First Medical University, 324 Jingwu Weiqi Road, Jinan, Shandong 250021, P.R. China
E-mail: liffchen@163.com

Key words: CD47, doxorubicin, dilated cardiomyopathy, cardiomyocytes, apoptosis

Introduction

Dilated cardiomyopathy (DCM) is a type of heart disease characterized by ventricular dilation along with impaired contractility, chronic inflammation and subsequent heart failure (1-3). There are no effective therapeutics for the disease thus far. Long-term use of anthracycline antibiotics and cytotoxic (antineoplastic) antitumor agents, such as doxorubicin (Dox), are major causes of the development of DCM, even 10-20 years after Dox chemotherapy has ceased (4). Gradual loss of cardiomyocytes over time and compensatory hypertrophic remodeling may contribute to the delayed onset of DCM. It has been documented that Dox enhances oxidation and DNA damage, and increases the accumulation of cytochrome *c*, myocardial apoptosis and pyroptosis. The expression of NAD(P)H oxidase, hydrogen peroxide, pro-apoptotic caspase-9, caspase-3, caspase-1, high-mobility group box 1 (HMGB1) and NLRP3 are increased in Dox-treated cardiomyocytes (5-8). However, the expression of anti-apoptotic Bcl-xL is reduced in Dox-treated cardiomyocytes (9-11).

Cluster of differentiation 47 (CD47) is a transmembrane glycoprotein that plays a complex role in the modulation of stem cells (12) and endothelial cell renewal (13). In addition, CD47 is upregulated in most types of tumors and participates in tumor immune evasion by suppressing macrophage efferocytosis of tumor cells and reducing tumor angiogenesis through interaction with thrombospondin-1 (14,15). It has been reported that the blockade of CD47 signaling significantly suppresses tumor cell survival and facilitates Dox-mediated antitumor effects *in vivo* (16-19). In addition, blockade of CD47 signaling can increase graft survival in recipients transplanted with CD47-knockout donor grafts (20). A previous study also revealed that CD47 is involved in the development of cardiovascular diseases. For example, CD47 expression was found to be upregulated in patients with clinical pulmonary hypertension, which was associated with pulmonary arterial vasculopathy and dysfunction (21). Furthermore, a lack or blockade of CD47 signaling was reported to significantly attenuate pulmonary hypertension and myocyte hypertrophy in mice, which was accompanied

by reduced expression of histone deacetylase 3 (HDAC3) and elevated expression of transcription factor c-Myc (21,22). In addition, the beneficial effects have been observed in animal models with ischemia-reperfusion injury, in which blocking CD47 signaling by small interfering (si)RNA or CD47 gene deficiency can effectively attenuate myocardial damage and increase the clearance of apoptotic cardiomyocytes (23,24). Studies in mice with isoproterenol-induced cardiac hypertrophy also showed these beneficial effects, in which anti-CD47 neutralizing antibody (aCD47) effectively suppressed cardiac hypertrophy and cardiac fibrosis (25).

Therefore, CD47 plays a critical role in the development of cardiovascular diseases. However, it is not fully understood whether CD47 signaling participates in the development of DCM in mice and the underlying molecular mechanisms remain elusive. Recently, Feliz-Mosquea *et al* (16) reported that targeting CD47 enhanced Dox-induced growth delay of tumors, while protecting cardiac tissue viability and function in mice. These beneficial effects were associated with the increased activation of protective autophagy and autophagic disposal of DOX-damaged mitochondria by aCD47 (16). This dual role in protecting cardiac tissues and improving antitumor effects was also observed in mice treated with phosphoinositide 3-kinase γ (PI3Kγ) inhibitor (26). In the present study, we aimed to explore the expression and role of CD47 in a mouse model with DCM. The results showed that blockade of CD47 signaling by aCD47 significantly attenuated myocardial cytotoxicity, which was associated with attenuated myocardial inflammation, cardiomyocyte early apoptosis and activation of p38 MAPK signaling. Therefore, CD47 appears to be a promising therapeutic target in DCM.

Materials and methods

Chemicals and reagents. Dox was purchased from MedChemExpress LLC. Anti-CD47 neutralizing antibody (aCD47) was purchased from Bio X Cell. ELISA kits for mouse tumor necrosis factor (TNF)-α and interleukin (IL-6) were purchased from R&D Systems. BCA assay kit was purchased from Thermo Fisher Scientific, Inc. Antibodies for flow cytometry staining, including purified rat anti-mouse CD16/CD32 (mouse Fc block; cat. no. 553141), APC-anti-mouse CD11b (cat. no. 101211), FITC-anti-mouse CD47 (cat. no. 127503) and PE-Cy7-anti-mouse Ly6G (cat. no. 560601) were purchased from BD Biosciences and BioLegend. The PE-Annexin V apoptosis detection kit was purchased from BioLegend. Anti-cardiac troponin T monoclonal antibody (cTnT, 13-11, (cat. no. MA5-12960), anti-collagen I (cat. no. ab21286), anti-Bax (cat. no. ab3191), anti-Bcl-2 (cat. no. ab16904), anti-cleaved caspase-1 and -3 (cat. nos. 9661 and 89332), and anti-p-p38 MAPK antibodies (cat. no. 9211) were purchased from Thermo Fisher Scientific, Abcam and Cell signaling, respectively. Cy3- or FITC-conjugated secondary antibodies were purchased from Jackson ImmunoResearch Laboratories (cat. nos. 711-165-152 and 715-165-150). Lactate dehydrogenase (LDH) activity assay kit was purchased from Beijing Solarbio Science & Technology.

Mice and treatment. A total of 63 male C57BL/6 mice (wild-type; 8-12 weeks of age; weight 18-22 g) were purchased from Shanghai Model Organisms Center (Shanghai, China), and housed in an animal facility at 23˚C (room temperature). All mice were maintained under a constant 12 h light-dark cycle and a standard mouse diet with *ad libitum* access to food and water. During the animal experiments, a mouse model of DCM was established by intraperitoneal (i.p.) administration of 5, 10 and 20 mg/kg Dox respectively for consecutive 4 weeks, according to the previous protocols with some modifications (1,27). For therapeutic treatment, murine DCM were i.p. treated with different doses of aCD47 (3.5, 7 and 14 mg/kg) weekly in 200 μl volume, according to a previous protocol with some modifications (17). Mice injected with PBS, aCD47 (7 mg/kg), or both Dox and goat IgG isotype in the same volume were used as the PBS, aCD47 and IgG/Dox control groups, respectively. The mice were sacrificed under anesthesia by i.p. injection of 75 mg/kg pentobarbital 4 weeks after treatment. Blood (150 μl) was collected via cardiac puncture and the hearts were removed for analysis. All animals were housed and treated according to the guidelines of the Institutional Animal Care and Use Committee of Fudan University, Zhongshan Hospital (Shanghai, China). The study protocol was approved by the Animal Experimental Ethics Committee of Zhongshan Hospital, Fudan University (Shanghai, China).

Echocardiography. A high-resolution micro-ultrasound system equipped with a 30-MHz probe (RMVTM 707b) was used for transthoracic echocardiography on mice. Briefly, the mice were anesthetized with 1.5% isoflurane and hearts were imaged in the two-dimensional parasternal short-axis view. M-mode echocardiogram of the mid-ventricle was recorded. The following measurements were obtained during both systole and diastole: heart rate, ejection fraction (EF), left ventricular fractional shortening (LVFS), left ventricular internal diameter (LVID), left ventricular posterior wall thickness (LVPW) and inter-ventricular septal thickness (IVS).

Heart histology and immunohistology. Heart tissues were fixed by 4% paraformaldehyde and processed for sectioning after paraffin embedding. Hematoxylin and eosin (H&E) and Masson staining were performed by standard protocols routinely used in our laboratory. The area of cardiomyocytes in H&E-stained heart tissues was semi-quantified by manual counting of center nuclei localized cardiac myofibers. Briefly, H&E-stained sections were viewed under a contrast microscope with x200 magnification. The entire cardiomyocytes were marked, and its area was measured. At least 10 randomly selected fields per section were marked and counted. The expression levels of collagen I and Bax in heart tissues were analyzed by immunostaining. Briefly, heart sections were incubated with 10% goat serum for 1 h, followed by incubation with 0.5% Triton X-100 for 10 min. Then, the sections were incubated with antibodies against collagen I and Bax (1:300 dilution, cat. nos. ab21286 and ab3191) overnight, followed by incubation with Cy3-conjugated secondary antibody (1:500 dilution, cat. no. 711-165-152). Nuclei were stained with 4',6-diamidino-2-phenylindole (DAPI). The stained sections were visualized under fluorescence microscope and semi-quantified by ImageJ software, v. 1.8.0 (National Institutes of Health).

Analysis of cytokines and LDH release. The expression of TNF-α and IL-6 in heart protein extracts and serum were measured by ELISA, according to the manufacturer's instructions. Briefly, 96-well Nunc MaxiSorp™ flat-bottom plates (Thermo Fisher Scientific, Inc.) were coated with 2 μg/ml capture antibody in coating buffer (0.1 M carbonate, pH 9.5) overnight. After incubation with blocking buffer [3% bovine serum albumin (BSA) in PBS], the plates were incubated with protein samples for 2 h, followed by incubation with 0.2 μg/ml biotin-conjugated detection antibody and streptavidin at the recommended concentration. After washed with washing buffer (PBS supplemented with 3% BSA and 0.05% Tween-20), the plates were developed using substrate TMB (3,3',5,5'-tetramethylbenzidine). The reaction was halted by 2N H_2SO_4, and absorbance was read by a spectrometer at 450 nm. LDH release was measured by using commercial kits (cat. no. BC0680), according to the manufacturer's instructions.

Flow cytometry analysis. Single cell suspensions were incubated with an antibody cocktail containing APC-anti-CD11b, FITC-anti-CD47 and PE-Cy7-anti-Ly6G for 30 min at room temperature. For blockade of Fc receptors on monocyte/macrophages and neutrophils during flow cytometric analysis, the cells were pre-incubated with 0.5 μg purified rat anti-CD16/CD32 for 5 min on ice prior to staining with antibody cocktail. Apoptotic cells were detected by PE-Annexin V apoptosis detection kit (BioLegend; cat. no. 640934), according to the manufacturer's recommendations. All stained cells were analyzed on a BD FACSAria™ III instrument (BD Biosciences) and FlowJo software, v. 8.8.4 (FlowJo LLC).

Cardiomyocyte isolation and immunostaining. Neonatal cardiomyocytes were isolated and cultured as previously described with some modifications (28). Briefly, wild-type C57BL/6 neonatal mice (1-3 g weight) were obtained from the mother 2-7 days after delivery and sacrificed by cervical dislocation. The hearts were collected and digested using 1 mg/ml collagenase A for 1 h at 37˚C. Primary cardiomyocytes were enriched by a pre-plating approach to remove contaminated cells before seeding into cell culture plates. The enriched cardiomyocytes were identified using a cTnT antibody and 95% purity of the cells was obtained. After 2 days in culture, cardiomyocytes were pre-treated with 1 μg/ml aCD47 for 1 h, followed by incubation with 10 μM Dox for 24 h. Anti-Bax (cat. no. ab3191), anti-Bcl-2 (cat. no. ab16904), anti-cleaved caspase-1 and -3 (cat. nos. 9661 and 89332), and anti-p-p38 MAPK (cat. no. 9211) antibodies (1:300 dilution) were used as primary antibodies. Cy3-conjugated anti-rabbit or mouse IgG (1:500 dilution; cat. nos. 711-165-152 and 715-165-150) were used as secondary antibodies. Nuclei were stained with DAPI. The positively stained cells (red) were visualized under a fluorescence microscope. Images were captured in 5 randomly selected fields at x200 magnification, and positively stained cells were semi-quantified by ImageJ software, v. 1.8.0. after images were inverted.

Western blot analysis. Protein expression of collagen I, Bax, Bcl-2, pro-caspase-1, cleaved caspase-1 and cleaved caspase-3 in the heart tissues and cells were analyzed via western blotting. Briefly, 40 μg protein samples were resolved on 10% SDS-PAGE gel. After running for 1 h at 100 V, the resolved protein was transferred onto a polyvinylidene fluoride membrane (EMD Millipore). Blots were then blocked with 3% non-fat milk for 30 min, followed by incubation with the indicated primary antibodies (1:1,000) for 2 h. The blots incubated with anti-GAPDH antibody (1:1,000 dilution; cat. no. ab9485) was used as a loading control. After washing with 1X Tris-buffered saline buffer with 0.05% Tween-20 (TBST), the blots were incubated with HRP-conjugated secondary antibody (1:1,000 dilution; cat. nos. 615-035-214 and 711-035-152) for 1 h. After washing with 1X TBST three times, immune reactivity was visualized using the enhanced chemiluminescent reagent (ECL) (Beyotime Institute of Biotechnology). Band densitometric intensity was semi-quantified by ImageJ software.

Statistical analysis. Results are presented as mean ± standard error, n=5-7. All data were first tested for normal distribution using the Shapiro-Wilk test (GraphPad Prism version 8.0.2, GraphPad Software, Inc.). Datasets of multiple groups passing the Shapiro-Wilk test were analyzed by one-way ANOVA followed by Tukey's multiple comparisons. Data that did not pass the Shapiro-Wilk test were analyzed by Mann Whitney test. $P<0.05$ was considered to be a statistically significant difference.

Results

CD47 is upregulated in the heart tissues of Dox-treated mice. Murine models of Dox-induced DCM were established by administration of 5 or 10 mg/kg Dox i.p. once a week for 4 weeks. After Dox treatment, we observed the increased number of cardiomyocytes in heart tissues of the treated mice, that was identified by center nuclei localized cells (red arrow) and broken cardiac myofibers (blue arrow) (Fig. 1A). In addition, Dox treatment upregulated CD47 expression in $CD11b^-$ cardiac myofibers and elevated the percentage of Annexin $V^+7\text{-}AAD^-$ early apoptotic cells in a dose-dependent manner (Fig. 1B). The detrimental effects were further observed in primary cardiomyocytes isolated from wild-type neonatal mice, in which the expression of CD47 in $CD11b^-$ cardiomyocytes was increased in a Dox concentration-dependent manner, as determined by flow cytometry analysis (Fig. 1C and D). Consistently, cell viability was gradually reduced in a Dox concentration-dependent manner (Fig. 1E). The results indicate the role of Dox in the upregulation of CD47 and the induction of cytotoxic effects.

aCD47 significantly reduces the severity of DCM. To further define whether blockade of CD47 signaling affects the development of DCM, mice were treated with 7 mg/kg aCD47 (i.p.) once a week in conjunction with 10 mg/kg Dox. We did not observe any abnormal heart morphology between the mice treated with PBS control and aCD47 alone, indicating that aCD47 had no obvious side effects on mice 4 weeks after aCD47 treatment. However, there was increased left ventricular chamber (LV) with thinned posterior wall in the Dox-treated mice, that was effectively reversed in the aCD47 co-treated mice, compared to the IgG-treated control [Fig. 2A (upper panel)]. M-mode non-invasive transthoracic

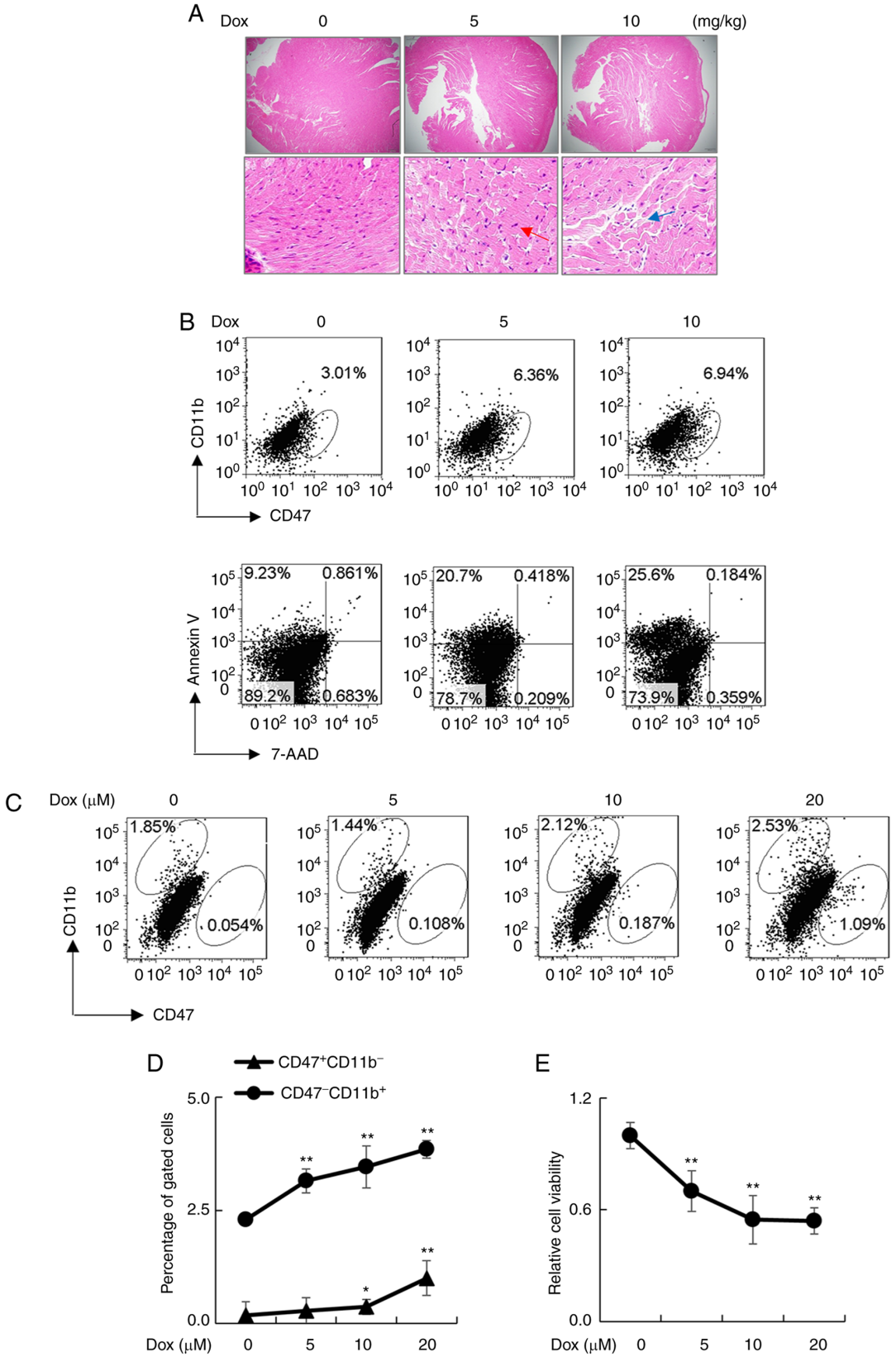

Figure 1. CD47 is upregulated in cardiomyocytes after Dox treatment. Adult mice were intraperitoneally (i.p.) administered with 5 and 10 mg/kg Dox once a week for 4 weeks. Mice treated with PBS were naïve controls. (A) Heart histology was analyzed by hematoxylin and eosin (H&E) staining. Representative images with x40 (upper panel) and x200 (lower panel) magnification. Red arrow, cardiomyocytes with centrally localized nuclei; blue arrow, broken myofibers. (B) Flow cytometry analysis for the expression of CD47 on $CD11b^-$ myofibers (upper panel) and Annexin $V^+7\text{-}AAD^-$ apoptotic myofibers (lower panel) in the cardiac tissues of treated mice. One representative dot plot of flow cytometry analysis. (C) Representative dot plot of flow cytometry analysis for CD47 expression 24 h after treatment of primary cardiomyocytes with different concentrations of Dox. (D) Quantitative analysis of CD47 expression on $CD11b^-$ cardiomyocytes and $CD11b^+$ immune cells after treatment with different concentrations of Dox. Data are presented as the mean percentage of gate cells ± standard error. $^*P<0.05$, $^{**}P<0.01$ vs. untreated control, n=3. Two-way ANOVA with Tukey's multiple comparison's test. (E) Viability of cardiomyocytes was measured by Cell Counting kit-8 (CCK-8) after Dox treatment *in vitro*. Data are presented as the mean optical density over untreated controls ± standard error. $^{**}P<0.01$ vs. untreated control, n=3. Two-way ANOVA with Tukey's multiple comparison's test. Dox, doxorubicin.

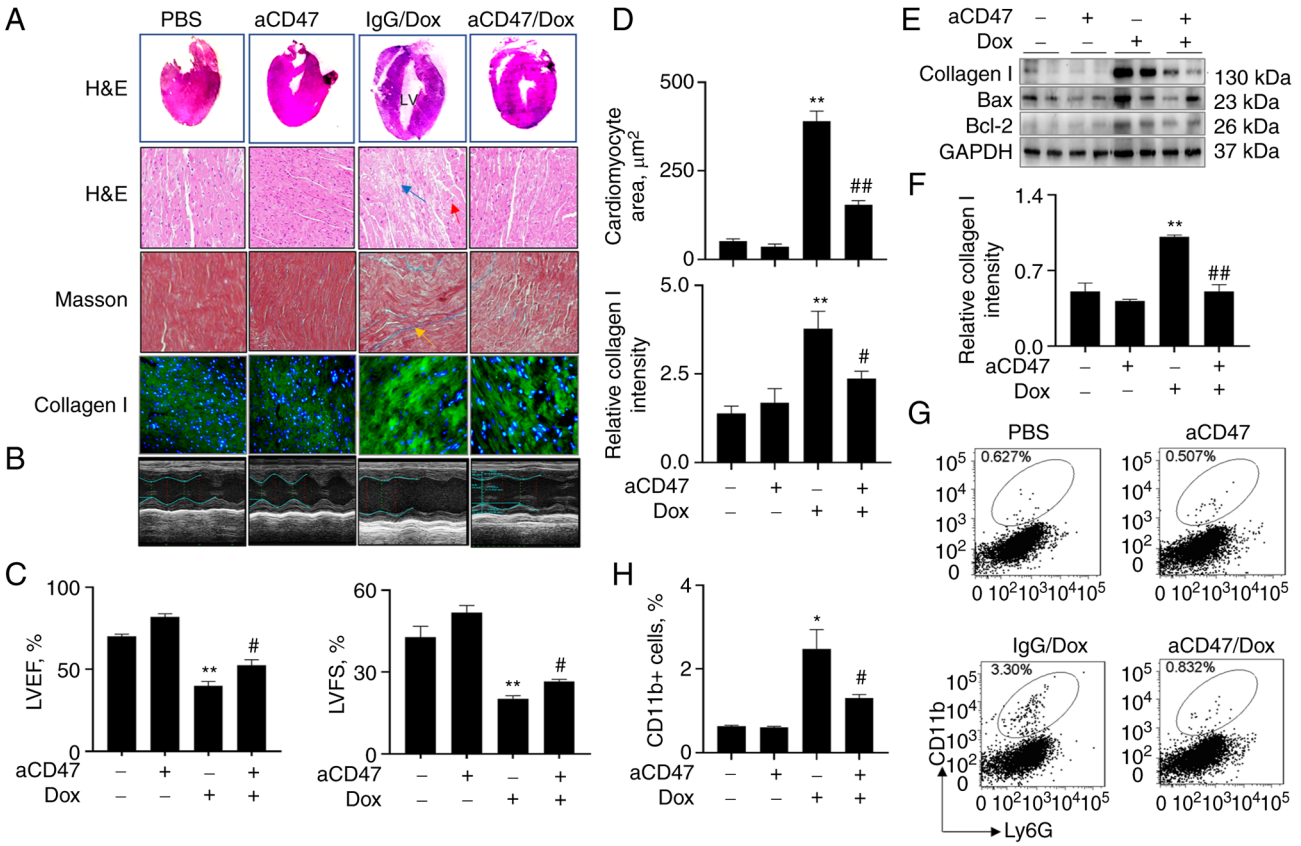

Figure 2. aCD47 significantly reduces the severity of Dox-induced dilated cardiomyopathy (DCM) in mice. Adult mice (aCD47/Dox group) were i.p. administered with both 7 mg/kg aCD47 and 10 mg/kg Dox once a week for 4 weeks. Mice treated with both IgG isotype and Dox (IgG/Dox group) or PBS and aCD47 alone (PBS and aCD47 groups) were controls. (A) Hematoxylin and eosin (H&E) staining for mouse heart tissues. Representative gross morphology and phase contrast microscope images with x200 magnification (upper two panels). Masson staining for interstitial fibrosis and immunostaining for collagen I (lower two panels). Representative images with x200 magnification. Red arrow, cells with centrally localized nuclei; blue arrow, broken and patchy myofibers; yellow arrow, interstitial fibrosis; green, collagen I. (B) Representative echocardiograms of mice 4 weeks after treatment. (C) Quantitative analysis of echocardiographic measurements. Left ventricular ejection fraction (LVEF); left ventricular fractional shortening (LVFS). (D) Quantitative analysis of cardiomyocyte area after H&E staining (upper panel; Mann-Whitney test) and fluorescence intensity of collagen I-positive fibers in heart tissues after immunostaining by ImageJ software. Data are presented as relative fluorescence intensity of positively stained cells over untreated controls. (E) Western blot analysis for the expression of collagen I, Bax and Bcl-2 in the cardiac tissues of treated mice. GAPDH was internal loading control. One representative blot. (F) Band densitometric intensity was semi-quantified by ImageJ software. (G) Flow cytometry analysis for the infiltrating CD11b$^+$ macrophages in cardiac tissues. (H) The infiltrating CD11b$^+$ macrophages in cardiac tissues were measured by flow cytometry and quantitatively analyzed. All quantitative data are presented as mean ± standard error. *P<0.05, **P<0.01 vs. PBS group; $^{\#}$P<0.05, $^{\#\#}$P<0.01 vs. IgG/Dox group (n=5-7). Two-way ANOVA with Tukey's multiple comparison's test, except where it is indicated otherwise. aCD47, anti-CD47 neutralizing antibody; Dox, doxorubicin.

echocardiography analysis revealed that both left ventricular ejection fraction (LVEF) and left ventricular fractional shortening (LVFS) were significantly improved in mice after aCD47 co-treatment, compared with the IgG-treated control mice, indicating successful establishment of murine DCM and beneficial effects of aCD47 on recovery of heart function in murine DCM (Fig. 2B and C). Further histological analysis of the heart tissues showed that aCD47 co-treatment significantly reduced hypertrophic cardiomyocytes (red arrow) and broken cardiac myofibers (patchy area, blue arrow), compared with the IgG-treated mice [Fig. 2A (upper panels) and D]. In addition, aCD47 co-treatment effectively reduced interstitial fibrosis (yellow arrow) and the expression of collagen I (green) in the heart tissues, compared with the IgG-treated murine DCM [Fig. 2A and D (lower panels)]. The suppressive effects of aCD47 on the expression of collagen I in the heart tissues of murine DCM were further confirmed via western blot analysis (Fig. 2E and F). Additional flow cytometry analysis also confirmed that infiltration of CD11b$^+$ macrophages were significantly reduced in the heart tissues of murine DCM after aCD47 treatment (Fig. 2G and H). The results indicated that aCD47 effectively suppressed the development of murine DCM, in association with the reduced interstitial fibrosis and infiltration of inflammatory cells in the heart tissues.

aCD47 suppresses cardiac myofiber early apoptosis in mice after Dox treatment. To further investigate the effects of aCD47 on cardiac myofiber apoptosis in murine DCM, mice were treated with Dox in conjunction with different doses of aCD47. Heart tissues were collected 4 weeks after co-treatment. We found an average of 40% Annexin V$^+$7-AAD$^-$ early apoptotic cardiac myofibers in the heart tissues of Dox-treated mice. There was no obvious Annexin V$^+$7-AAD$^-$ early apoptotic cardiac myofibers in the heart tissues of mice treated with aCD47 alone, indicating no potential side effects of aCD47 in mice. In addition, we observed that aCD47 co-treatment exhibited effective suppressive effects on early apoptosis of cardiac myofiber in murine DCM (Fig. 3A and B). aCD47

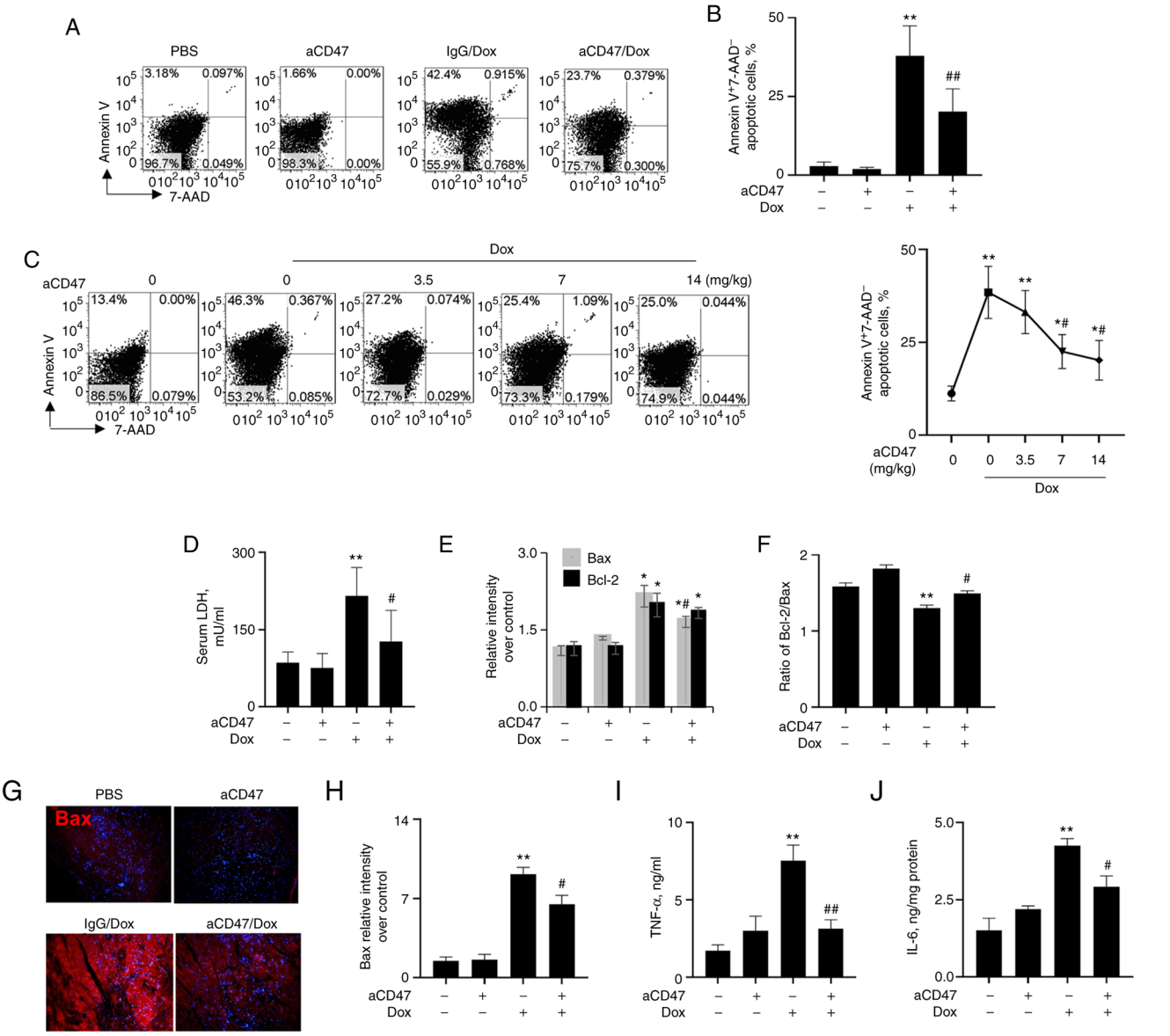

Figure 3. aCD47 suppresses the expression of cardiac myofiber early apoptosis and production of pro-inflammatory cytokines in mice with Dox-induced DCM. (A) Cardiac myofiber apoptosis in the treated mice was analyzed by flow cytometry analysis. Annexin V$^+$7-AAD$^-$ cells were identified as early apoptotic cells. Annexin V$^+$7-AAD$^+$ cells were identified as late apoptotic cells. Representative dot plot. (B) Quantitative analysis of apoptotic cells after flow cytometry analysis. **P<0.01 vs. untreated mice; $^{\#\#}$P<0.05 vs. mice treated with Dox alone, n=5-7. Two-way ANOVA with Tukey's multiple comparison's test. (C) Different doses of aCD47 (3.5, 7 and 14 mg/kg) on apoptosis of cardiac myofiber in mice with DCM. Representative dot plot (left panel). Quantitative analysis of early apoptotic cells (right panel). *P<0.05 and **P<0.01 vs. untreated mice; $^{\#}$P<0.05 vs. mice treated with Dox alone (Dox/0 group), n=3/group. Two-way ANOVA with Tukey's multiple comparison's test. (D) Measurement of LDH release in serum. Data are presented as mean ± standard error (Mann-Whitney test). (E) Quantitative analysis of Bax and Bcl-2 expression in cardiac tissues of treated mice in Fig. 2E. Data are presented as the ratio of band densitometric intensity over untreated control. (F) Ratio of Bcl-2/Bax expression in lung tissues of treated mice analyzed by western blot analysis in Fig. 2E. (G) Immunostaining for Bax (red) in the cardiac tissues of treated mice. Representative images with x200 magnification. (H) Quantitative analysis for Bax expression in the stained cells by ImageJ software. Data are presented as the fluorescence intensity over controls. (I and J) ELISA analysis for the expression of TNF-a in serum and IL-6 in heart protein extracts. Data are presented as mean ± standard error. **P<0.01 vs. PBS group; $^{\#}$P<0.05, $^{\#\#}$P<0.01 vs. IgG/Dox group (n=5-7). Two-way ANOVA with Tukey's multiple comparison's test, except where it is indicated otherwise. aCD47, anti-CD47 neutralizing antibody; Dox, doxorubicin; LDH, lactate dehydrogenase.

suppressed early apoptosis of cardiac myofiber in murine DCM at a dose-dependent manner with a plateau at weekly doses of aCD47 over 7 mg/kg aCD47 (Fig. 3C). In addition, we observed that LDH release was significantly attenuated in the aCD47-treated mice, compared with the IgG-treated controls (Fig. 3D). Further analysis via western blotting indicated that Dox effectively upregulated the expression of both Bax and Bcl-2, and these were significantly reduced by aCD47 co-treatment, with more reduced expression of Bax than Bcl-2 and increased ratio of Bcl-2/Bax after aCD47 co-treatment (Figs. 2E and 3E and F). These results were further demonstrated by immunostaining of heart tissues, in which the expression of both Bax (Fig. 3G and H) and Bcl-2 (data not shown) was upregulated by Dox, which was reversed by aCD47 co-treatment. In addition, we observed the significantly elevated expression of pro-inflammatory cytokines, including TNF-α and IL-6 in the heart tissues of Dox-treated mice, which was effectively attenuated by aCD47 co-treatment

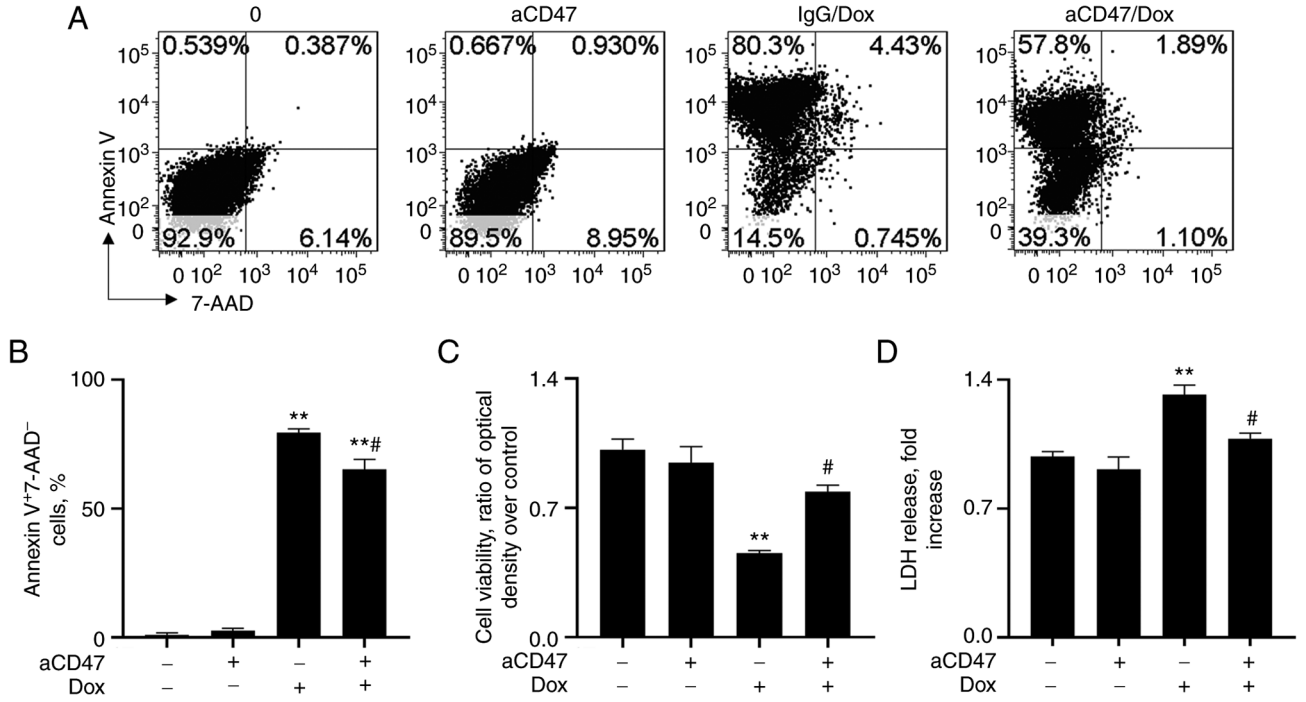

Figure 4. aCD47 reduces Dox-induced cardiomyocyte early apoptosis. The cultured primary cardiomyocytes were pre-treated with 1 μg/ml aCD47 for 1 h, which was followed by treatment with 10 μM Dox (aCD47/Dox group) for 24 h. The cells treated with both Dox and isotype IgG (IgG/Dox), untreated or treated with aCD47 alone (aCD47 group) were controls. (A) Flow cytometry analysis for Annexin V$^+$7-AAD$^-$ apoptotic cardiomyocytes 24 h after treatment. Representative dot plots. (B) Quantitative analysis for apoptotic cardiomyocytes analyzed by flow cytometry. (C) Cell viability was determined by CCK-8 assay. Data are presented as the ratio of optical density at 450 nm (OD450 nm) over untreated control. (D) LDH release into the supernatant of the treated cells. Data are presented as the fold increase over untreated controls. Bar plot data in all panels represent the mean ± standard error. n=3. **P<0.01 vs. 0 group; $^{\#}$P<0.05 vs. IgG/Dox group. Two-way ANOVA followed by a Tukey's multiple comparison's test. aCD47, anti-CD47 neutralizing antibody; Dox, doxorubicin; LDH, lactate dehydrogenase.

(Fig. 3I and J). Therefore, aCD47 attenuated the severity of DCM, in association with the reduced cardiac myofiber early apoptosis and expression of pro-inflammatory cytokines in heart tissues.

aCD47 reduces cardiomyocyte early apoptosis in vitro. To investigate whether the reduced severity of DCM by aCD47 was caused by targeting CD47 on cardiomyocytes, primary cardiomyocytes from neonatal mice were treated with 1 μg/ml aCD47, in conjunction with 10 μM Dox for 24 h. The results of flow cytometry analysis showed that Dox treatment effectively increased Annexin V$^+$7-AAD$^-$ cardiomyocyte early apoptosis, which was significantly reversed by pre-treatment with aCD47 (Fig. 4A and B). Consistently, aCD47 co-treatment effectively improved cell viability and attenuated LDH release into the cell supernatants, compared with the IgG co-treated control cells (Fig. 4C and D). The results indicated the direct anti-apoptotic effects of aCD47 on cardiomyocytes.

aCD47 reduces cardiomyocyte early apoptosis by suppressing the expression of Bax and p38 MAPK signaling. Immunostaining showed that the isolated cardiomyocytes were stained positive for cTnT, a cardiomyocyte-specific marker, confirming that the isolated cells were indeed cardiomyocytes [Fig. 5A (upper panel, green)]. Treatment with aCD47 and Dox did not change the expression of cTnT, indicating no effects of aCD47 on cardiomyocyte proliferation and differentiation. However, as expected, we observed the increased expression of cleaved caspase-1, cleaved caspase-3 and Bax in the Dox-treated cardiomyocytes, which was effectively reversed by aCD47 pre-treatment [Fig. 5A (middle panel) and B]. The results were further confirmed by western blot analysis, in which aCD47 pre-treatment effectively suppressed Dox-induced upregulation of cleaved caspase-1, cleaved caspase-3 and Bax (Fig. 5C). The expression of Bcl-2 was upregulated in cardiomyocytes by treatment of Dox alone or in conjunction with both Dox and aCD47. aCD47 and Dox co-treatment induced increased upregulation of Bcl-2 when compared with Dox treatment alone (Fig. 5C), indicating the synergistic effects of aCD47 and Dox in increasing the expression of Bcl-2. The effects induced an increased ratio of Bcl-2/Bax in the aCD47 cotreated cardiomyocytes.

To further investigate the downstream signaling pathway of aCD47-mediated suppression of cardiomyocyte early apoptosis, the activation of p38 MAPK in the treated cells was further measured. The results by immunostaining [Fig. 5A (lower panel) and B (right lower panel)] indicated that Dox significantly increased p-p38 MAPK, which was significantly reversed by co-treatment with aCD47 in the aCD47/Dox group. Further analysis by flow cytometry confirmed the attenuated percentage of p-38 MAPK$^+$ cells in aCD47/Dox co-treated cells, compared to Dox alone-treated controls (Fig. 5D). There was a positive association between the percentage of p-p38 MAPK$^+$ cells and cardiomyocyte

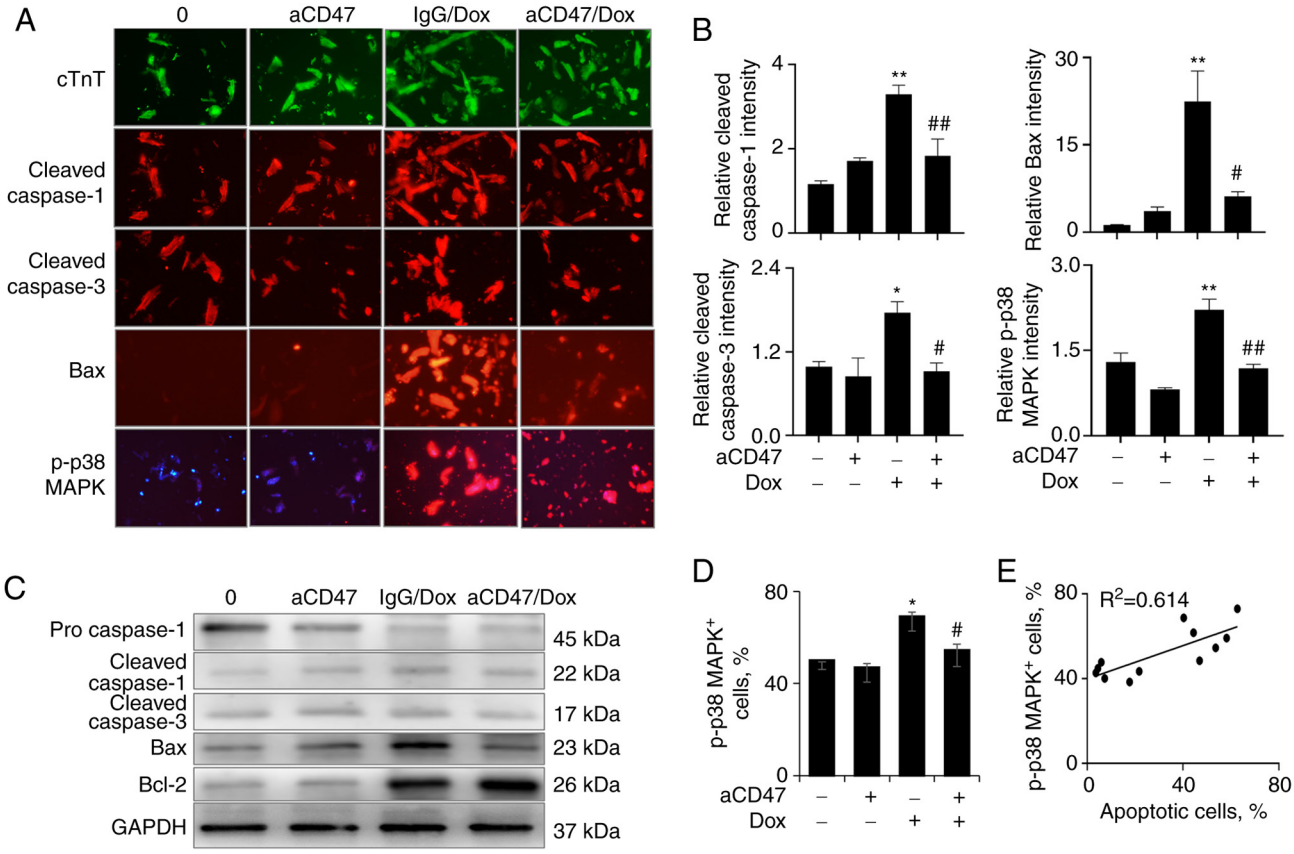

Figure 5. aCD47 reduces the expression of Bax and p-p38 MAPK in Dox-treated cardiomyocytes. (A) Immunostaining for the expression of cTnT, cleaved caspase-1/3, Bax and p-p38 MAPK in the treated cardiomyocytes. Cardiomyocytes were identified as cTnT-positive cells (green). Red, cells positively stained for cleaved caspase-1/3, Bax and p-p38 MAPK. Representative images with x200 magnification. (B) Semi-quantitative analysis of positively stained cells by ImageJ software. Data are presented as the relative intensity of positively stained cells over untreated controls. (C) Western blot analysis for the expression of pro-caspase-1, cleaved caspase-1, cleaved caspase-3, Bax and Bcl-2 in the treated cardiomyocytes. GAPDH was internal loading control. One representative blot. (D) p-p38 MAPK$^+$ cells after Dox and aCD47 treatment were analyzed by flow cytometry. Data are presented as the percentage of p-p38 MAPK$^+$ cells. (E) Association between the percentage of p-p38 MAPK$^+$ cells and apoptotic cardiomyocytes after treatment. Bar plot data in all panels are represented as mean ± standard error. n=3. *P<0.05, **P<0.01 vs. 0 group; $^{\#}$P<0.05, $^{\#\#}$P<0.01 vs. IgG/Dox group. Two-way ANOVA followed by a Tukey's multiple comparison's test. aCD47, anti-CD47 neutralizing antibody; Dox, doxorubicin; p-, phosphorylated; cTnT, cardiac troponin T.

early apoptosis (Fig. 5E). These results indicate that p38 MAPK signaling was involved in the aCD47-mediated protection against Dox-induced cardiomyocyte early apoptosis.

Discussion

CD47 is expressed at low levels in normal human tissues. However, recent studies have shown that the expression of CD47 is increased in atherosclerosis (29), pathogen-infected cells (30) and tumors (18,31). The upregulated expression of CD47 on cells can interact with signal regulatory protein-a (SIRP-a) on macrophages or natural killer cells, subsequently suppressing phagocytosis of macrophages and reducing the clearance of apoptotic cells, dead cells and tumor cells. Therefore, targeting CD47 is a promising therapeutic approach to improving tissue repair and inflammation resolution. It was recently reported that blocking CD47 activity by aCD47 or CD47 deficiency effectively suppressed isoproterenol-induced cardiac hypertrophy and protected cardiomyocytes from hypoxia/reoxygenation-induced cardiac injury by suppressing cell apoptosis, as well as improving autophagic flux and autophagic clearance (23,25).

Consistent with the upregulated CD47 expression in atherosclerosis and pulmonary hypertension (21,29,32), the results of the present study showed that CD47 expression was increased in the mice with Dox-induced dilated cardiomyopathy (DCM), suggesting the possible involvement of CD47 in the pathogenesis of murine DCM.

To further define the role of CD47 in the development of DCM, CD47 activity was blocked by i.p. administration of aCD47 to murine models of DCM for 4 weeks. The results revealed that aCD47 significantly reduced the severity of murine DCM, as evidenced by the reduced destruction of cardiac myofibers and formation of interstitial fibrosis in the myocardium. The beneficial effects were accompanied by reduced infiltration of macrophages and cardiac myofiber early apoptosis, as compared with the murine DCM treated with IgG isotype control. In addition, LDH release and the expression of pro-inflammatory cytokines, including IL-6 and TNF-α, were significantly reduced in aCD47-treated mice, confirming the anti-inflammatory effect of aCD47 in murine DCM. The reduced infiltration of inflammatory cells may contribute to the lower expression of pro-inflammatory cytokines and mediators *in vivo*. Supporting the anti-apoptotic and anti-inflammatory role of aCD47 in murine

DCM, similar beneficial effects have also been observed in other animal models, such as vascular inflammation (33), isoproterenol-induced heart hypertrophy (25), hypoxia/reoxygenation injury (23) and allograft transplantation (20). Therefore, CD47 is a promising target in the treatment of cardiovascular diseases. As there were no obvious effects of aCD47 on cardiac histology and myofiber apoptosis in the aCD47 alone-treated mice, it may be inferred that there are no toxic effects associated with the potential use of aCD47 in humans in the future. However, it should be noted that the study was limited by lack of time-point study for aCD47 therapeutic effects *in vivo*. In addition, an actual tumor model should be used in future study, as the tumor microenvironment may affect the therapeutic effects of aCD47 *in vivo*. A cardiomyocyte-specific CD47 knockout mouse model may be used to further dissect the role and underlying molecular mechanisms of CD47 in the pathogenesis of murine DCM.

At present, it remains unknown whether aCD47 suppresses DCM through directly targeting cardiomyocytes or indirectly suppressing the immune responses. To further address this issue, an *in vitro* experiment was performed in the current study, in which primary cardiomyocytes were treated with Dox and aCD47, alone or in combination. Consistent with the *in vivo* results, the increased cardiomyocyte early apoptosis and LDH release were observed after Dox treatment. However, aCD47 pre-treatment effectively reversed Dox-induced cardiomyocyte early apoptosis and LDH release, confirming the direct targeting of aCD47 on cardiomyocytes. Thus, Dox treatment upregulated the expression of CD47 and participated in the pathogenesis of murine DCM, and the detrimental effects were attenuated by blocking CD47 signaling with aCD47. Further analysis also indicated that Dox effectively upregulated the expression of both pro-apoptotic Bax and anti-apoptotic Bcl-2. However, Bax, but not Bcl-2, was effectively reversed by aCD47 pre-treatment *in vitro*, indicating the direct anti-apoptotic effect of aCD47 in Dox-treated cardiomyocytes. These results were consistent with previously reported results, in which cocaine treatment upregulated the expression of both Bcl-2 and Bax protein, with an increased ratio of Bax/Bcl-2 in neuronal cells (34). Thus, we speculate that the increased expression of Bcl-2 may play a protective feedback role in Dox-induced cardiomyocyte early apoptosis and aCD47 may protect cardiomyocytes from early apoptosis via increasing the ratio of Bcl-2/Bax.

In addition, the present study showed the increased phosphorylation of p38 MAPK in Dox-treated cardiomyocytes, but aCD47 pre-treatment effectively reduced the activation of p38 MAPK. As p38 MAPK signaling is associated with cardiomyocyte activation and apoptosis as previously reported (3,35-37), we concluded that aCD47 may suppress cardiomyocyte early apoptosis through blocking CD47 downstream p38 MAPK signaling pathway, and subsequently reducing the expression of pro-apoptotic protein Bax in cardiomyocytes.

It should not be excluded that aCD47 may target CD47 on other cell types, such as immune, vascular, epithelial and stem cells, improving angiogenesis and renal tubular epithelial cell renewal (12,13). For example, CD47 was highly expressed in animal models of pulmonary hypertension (PH), and blockade of CD47 signaling by CD47 antibody was able to effectively attenuate PH-associated cardiopulmonary pathological changes and enhance cell renewal (21). Thus, it was hypothesized that the improved cardiomyocyte renewal may be involved in the protective effects of aCD47 in murine DCM. It will be investigated further in the future.

Apoptotic and dead cells prevent tissue repair by stimulating local tissue inflammation. Effective clearance of apoptotic and dead cells may facilitate local inflammation resolution and tissue repair. It was previously reported that blockade of CD47 signaling effectively reduced atherosclerosis through improving the clearance of diseased vascular tissues (29,38). Therefore, it is hypothesized that aCD47 effectively attenuated DCM, possibly through improving the clearance of apoptotic cardiac myofibers and inflammatory cells in the heart tissues of murine DCM.

Taken together, the findings of the *in vivo* and *in vitro* experiments performed in the present study provide evidence that aCD47 attenuated DCM in mice, by suppressing cardiac myofiber early apoptosis and the p38 MAPK signaling pathway. CD47 may be a useful therapeutic target for Dox-induced DCM.

Acknowledgements

Not applicable.

Funding

This study was supported by a research grant from the Natural Science Foundation of Shanghai (19ZR1409000) to ZLJ.

Availability of data and materials

The datasets used and/or analyzed during the current study are available from the corresponding author on reasonable request.

Authors' contributions

YH designed and performed the experiments. LC generated the hypothesis and designed the study. ZJ was responsible for generating the hypothesis, performing the experiments, writing the manuscript and was responsible for all directions of the work. All authors confirm the authenticity of all the raw data. All authors read and approved the final manuscript for publication.

Ethics approval and consent to participate

The study protocol was approved by the Animal Experimental Ethics Committee of Zhongshan Hospital, Fudan University (approval number 20130039; 26/02/2020).

Patient consent for publication

Not applicable.

Competing interests

The authors declare that they have no competing interests.

References

1. Liu Y, Zhang W, Hu T, Ni J, Xu B and Huang W: A doxorubicin-induced murine model of dilated cardiomyopathy in vivo. J Vis Exp: May 16, 2020 (Epub ahead of print). doi: 10.3791/61158.
2. Rocca C, Scavello F, Colombo B, Gasparri AM, Dallatomasina A, Granieri MC, Amelio D, Pasqua T, Cerra MC, Tota B, *et al*: Physiological levels of chromogranin A prevent doxorubicin-induced cardiotoxicity without impairing its anticancer activity. FASEB J 33: 7734-7747, 2019.
3. Wang S, Ding L, Ji H, Xu Z, Liu Q and Zheng Y: The role of p38 MAPK in the development of diabetic cardiomyopathy. Int J Mol Sci 17: 1037, 2016.
4. Kankeu C, Clarke K, Passante E and Huber HJ: Doxorubicin-induced chronic dilated cardiomyopathy-the apoptosis hypothesis revisited. J Mol Med (Berl) 95: 239-248, 2017.
5. Cheng X, Liu D, Xing R, Song H, Tian X, Yan C and Han Y: Orosomucoid 1 attenuates doxorubicin-induced oxidative stress and apoptosis in cardiomyocytes via Nrf2 signaling. Biomed Res Int 2020: 5923572, 2020.
6. Song T, Yao Y, Wang T, Huang H and Xia H: Tanshinone IIA ameliorates apoptosis of myocardiocytes by up-regulation of miR-133 and suppression of caspase-9. Eur J Pharmacol 815: 343-350, 2017.
7. Yao Y, Xu X, Zhang G, Zhang Y, Qian W and Rui T: Role of HMGB1 in doxorubicin-induced myocardial apoptosis and its regulation pathway. Basic Res Cardiol 107: 267, 2012.
8. Zeng C, Duan F, Hu J, Luo B, Huang B, Lou X, Sun X, Li H, Zhang X, Yin S and Tan H: NLRP3 inflammasome-mediated pyroptosis contributes to the pathogenesis of non-ischemic dilated cardiomyopathy. Redox Biol 34: 101523, 2020.
9. Li J, Wang PY, Long NA, Zhuang J, Springer DA, Zou J, Lin Y, Bleck CKE, Park JH, Kang JG and Hwang PM: p53 prevents doxorubicin cardiotoxicity independently of its prototypical tumor suppressor activities. Proc Natl Acad Sci USA 116: 19626-19634, 2019.
10. Mizutani H, Tada-Oikawa S, Hiraku Y, Kojima M and Kawanishi S: Mechanism of apoptosis induced by doxorubicin through the generation of hydrogen peroxide. Life Sci 76: 1439-1453, 2005.
11. Reeve JL, Szegezdi E, Logue SE, Ní Chonghaile T, O'Brien T, Ritter T and Samali A: Distinct mechanisms of cardiomyocyte apoptosis induced by doxorubicin and hypoxia converge on mitochondria and are inhibited by Bcl-xL. J Cell Mol Med 11: 509-520, 2007.
12. Rogers NM, Zhang ZJ, Wang JJ, Thomson AW and Isenberg JS: CD47 regulates renal tubular epithelial cell self-renewal and proliferation following renal ischemia reperfusion. Kidney Int 90: 334-347, 2016.
13. Ghimire K, Li Y, Chiba T, Julovi SM, Li J, Ross MA, Straub AC, O'Connell PJ, Rüegg C, Pagano PJ, *et al*: CD47 promotes age-associated deterioration in angiogenesis, blood flow and glucose homeostasis. Cells 9: 1695, 2020.
14. Kaur S, Bronson SM, Pal-Nath D, Miller TW, Soto-Pantoja DR and Roberts DD: Functions of thrombospondin-1 in the tumor microenvironment. Int J Mol Sci 22: 4570, 2021.
15. Rath GM, Schneider C, Dedieu S, Rothhut B, Soula-Rothhut M, Ghoneim C, Sid B, Morjani H, El Btaouri H and Martiny L: The C-terminal CD47/IAP-binding domain of thrombospondin-1 prevents camptothecin- and doxorubicin-induced apoptosis in human thyroid carcinoma cells. Biochim Biophys Acta 1763: 1125-1134, 2006.
16. Feliz-Mosquea YR, Christensen AA, Wilson AS, Westwood B, Varagic J, Meléndez GC, Schwartz AL, Chen QR, Mathews Griner L, Guha R, *et al*: Combination of anthracyclines and anti-CD47 therapy inhibit invasive breast cancer growth while preventing cardiac toxicity by regulation of autophagy. Breast Cancer Res Treat 172: 69-82, 2018.
17. Lo J, Lau EY, So FT, Lu P, Chan VS, Cheung VC, Ching RH, Cheng BY, Ma MK, Ng IO and Lee TK: Anti-CD47 antibody suppresses tumour growth and augments the effect of chemotherapy treatment in hepatocellular carcinoma. Liver Int 36: 737-745, 2016.
18. Tong B and Wang M: CD47 is a novel potent immunotherapy target in human malignancies: Current studies and future promises. Future Oncol 14: 2179-2188, 2018.
19. Veillette A and Chen J: SIRPα-CD47 immune checkpoint blockade in anticancer therapy. Trends Immunol 39: 173-184, 2018.
20. Chen M, Wang Y, Wang H, Sun L, Fu Y and Yang YG: Elimination of donor CD47 protects against vascularized allograft rejection in mice. Xenotransplantation 26: e12459, 2019.
21. Rogers NM, Sharifi-Sanjani M, Yao M, Ghimire K, Bienes-Martinez R, Mutchler SM, Knupp HE, Baust J, Novelli EM, Ross M, *et al*: TSP1-CD47 signaling is upregulated in clinical pulmonary hypertension and contributes to pulmonary arterial vasculopathy and dysfunction. Cardiovasc Res 113: 15-29, 2017.
22. Sharifi-Sanjani M, Shoushtari AH, Quiroz M, Baust J, Sestito SF, Mosher M, Ross M, McTiernan CF, St Croix CM, Bilonick RA, *et al*: Cardiac CD47 drives left ventricular heart failure through Ca^{2+}-CaMKII-regulated induction of HDAC3. J Am Heart Assoc 3: e000670, 2014.
23. Li Y, Zhao K, Zong P, Fu H, Zheng Y, Bao D, Yin Y, Chen Q, Lu L, Dai Y, *et al*: CD47 deficiency protects cardiomyocytes against hypoxia/reoxygenation injury by rescuing autophagic clearance. Mol Med Rep 19: 5453-5463, 2019.
24. Wang HB, Yang J, Ding JW, Chen LH, Li S, Liu XW, Yang CJ, Fan ZX and Yang J: RNAi-mediated down-regulation of CD47 protects against ischemia/reperfusion-induced myocardial damage via activation of eNOS in a rat model. Cell Physiol Biochem 40: 1163-1174, 2016.
25. Li Y, Chen X, Li P, Xiao Q, Hou D and Kong X: CD47 antibody suppresses isoproterenol-induced cardiac hypertrophy through activation of autophagy. Am J Transl Res 12: 5908-5923, 2020.
26. Li M, Sala V, De Santis MC, Cimino J, Cappello P, Pianca N, Di Bona A, Margaria JP, Martini M, Lazzarini E, *et al*: Phosphoinositide 3-kinase gamma inhibition protects from anthracycline cardiotoxicity and reduces tumor growth. Circulation 138: 696-711, 2018.
27. Hu C, Zhang X, Wei W, Zhang N, Wu H, Ma Z, Li L, Deng W and Tang Q: Matrine attenuates oxidative stress and cardiomyocyte apoptosis in doxorubicin-induced cardiotoxicity via maintaining AMPKα/UCP2 pathway. Acta Pharm Sin B 9: 690-701, 2019.
28. Rui T, Cepinskas G, Feng Q and Kvietys PR: Delayed preconditioning in cardiac myocytes with respect to development of a proinflammatory phenotype: Role of SOD and NOS. Cardiovasc Res 59: 901-911, 2003.
29. Kojima Y, Volkmer JP, McKenna K, Civelek M, Lusis AJ, Miller CL, Direnzo D, Nanda V, Ye J, Connolly AJ, *et al*: CD47-blocking antibodies restore phagocytosis and prevent atherosclerosis. Nature 536: 86-90, 2016.
30. Tal MC, Torrez Dulgeroff LB, Myers L, Cham LB, Mayer-Barber KD, Bohrer AC, Castro E, Yiu YY, Lopez Angel C, Pham E, *et al*: Upregulation of CD47 is a host checkpoint response to pathogen recognition. mBio 11: e01293-20, 2020.
31. Deuse T, Hu X, Agbor-Enoh S, Jang MK, Alawi M, Saygi C, Gravina A, Tediashvili G, Nguyen VQ, Liu Y, *et al*: The SIRPα-CD47 immune checkpoint in NK cells. J Exp Med 218: e20200839, 2021.
32. Novelli EM, Little-Ihrig L, Knupp HE, Rogers NM, Yao M, Baust JJ, Meijles D, St Croix CM, Ross MA, Pagano PJ, *et al*: Vascular TSP1-CD47 signaling promotes sickle cell-associated arterial vasculopathy and pulmonary hypertension in mice. Am J Physiol Lung Cell Mol Physiol 316: L1150-L1164, 2019.
33. Jarr KU, Nakamoto R, Doan BH, Kojima Y, Weissman IL, Advani RH, Iagaru A and Leeper NJ: Effect of CD47 blockade on vascular inflammation. N Engl J Med 384: 382-383, 2021.
34. Xiao D and Zhang L: Upregulation of Bax and Bcl-2 following prenatal cocaine exposure induces apoptosis in fetal rat brain. Int J Med Sci 5: 295-302, 2008.
35. Cao Y, Ruan Y, Shen T, Huang X, Li M, Yu W, Zhu Y, Man Y, Wang S and Li J: Astragalus polysaccharide suppresses doxorubicin-induced cardiotoxicity by regulating the PI3k/Akt and p38MAPK pathways. Oxid Med Cell Longev 2014: 674219, 2014.
36. Xuan T, Wang D, Lv J, Pan Z, Fang J, Xiang Y, Cheng H, Wang X and Guo X: Downregulation of Cypher induces apoptosis in cardiomyocytes via Akt/p38 MAPK signaling pathway. Int J Med Sci 17: 2328-2337, 2020.
37. Zuo G, Ren X, Qian X, Ye P, Luo J, Gao X, Zhang J and Chen S: Inhibition of JNK and p38 MAPK-mediated inflammation and apoptosis by ivabradine improves cardiac function in streptozotocin-induced diabetic cardiomyopathy. J Cell Physiol 234: 1925-1936, 2019.
38. Gerlach BD, Marinello M, Heinz J, Rymut N, Sansbury BE, Riley CO, Sadhu S, Hosseini Z, Kojima Y, Tang DD, *et al*: Resolvin D1 promotes the targeting and clearance of necroptotic cells. Cell Death Differ 27: 525-539, 2020.